NUMERICAL STUDY OF FLUID ATOMIZATION IN A HIGH-VELOCITY SPRAY

Wei Wang[1,2], Steve Bajic[1], Benzi John[2], David Emerson[2]

[1]Waters Corporation, Altrincham Rd, Wilmslow, Cheshire, SK9 4AX, UK
[2]STFC Daresbury Laboratory, Warrington, Cheshire, WA4 4AD, UK

OVERVIEW

Numerical simulations were carried out to study flow dynamics, droplet formation and droplet transport in two gas-assisted nebulizers.

- **For typical operating conditions, both nebulizers produce strong shock diamonds and a high frequency of vortex shedding.**
- **The volume of fluid simulation of the nebulizer atomization shows that flow-blurring occurs in both nebulizers and the droplet generation frequency is strongly correlated with gas flow vortex shedding frequency.**
- **The simulation of the atomization process with the discrete phase model in ANSYS Fluent underestimates droplet size and gives a smaller relative span of droplet distribution.**

INTRODUCTION

Nebulizers play an important role in the ionization source of mass spectrometers. The high-velocity spray plume in nebulizers strongly influences the atomization of sample solutions, especially the primary droplet size distribution, which is an important step in the production of gas-phase ions for a mass spectrometer. It is desirable to predict gas flow properties of nebulizers in an ion source and understand their influence on droplet generation in a high-velocity spray. However, these tasks are challenging to achieve with laboratory experiments due to limited measurement techniques. In this study, a numerical simulation of the nebulizer gas flow fields was carried out. After achieving a fully developed nebulizer gas flow field, liquid injection through the capillary was modelled to study the droplet generation dynamics. Based on the initial liquid spray and liquid sheet information, simulation of droplet atomization (secondary breakup) was conducted to investigate the characteristics of droplets transport.

METHODS

ANSYS Fluent is applied to carry out simulations of high-speed nebulizer gas flow and liquid injection. Unsteady Reynolds Averaged Navier-Stokes (URANS) equations with the k-ω SST turbulence model are applied to simulate nebulizer gas flow. The transient simulation captures vortex shedding dynamics, which will strongly affect droplet generation once the liquid injection is introduced.

When the liquid flow is introduced, a volume of fluid (VOF) method is applied to model the two-phase flow of the injected liquid water and the nitrogen nebulizer gas. The continuum surface force method is applied to treat surface tension modelling. Local adaptive mesh refinement is enabled to ensure improved grid resolution at the gas-liquid interface.

Based on the VOF simulation results for the gas-liquid, i.e. relative velocity, spray angle and atomizer dispersion angle, the air-blast/air-assist atomizer model is used in the discrete phase method (DPM) simulation to track droplet transport. The current model uses two empirical parameters, sheet constant and ligament constant, which were originally obtained for liquid jets over a Weber number range of 2 to 200. The validity of this Weber number range for high velocity nebulizers will be tested in these simulations. The Kelvin-Helmholtz and Rayleigh-Taylor (KHRT) breakup model is applied to model droplet breakup in a higher Weber number spray.

RESULTS

Computational model and configuration

This study simulates flow fields, droplet generation and transport in two types of Meinhard® nebulizers, which are named “TR-50-A0.5” and “HEN-90-A0.1”. Their operation parameters [1] are summarized in Table 1. The listed dimensions were measured in-house.

A schematic of the computational domain is shown in Figure 1. A 2D axisymmetric CFD model is used to save computational cost. At the inlets of both the gas and liquid, mass flow rates and pressure are provided. The outer edges of the domain are given a boundary condition of atmospheric pressure.

Table 1. Nebulizer parameters

Nebulizer Type	TR-50-A0.5	HEN-90-A0.1
Operating pressure (psi)	50	90
Gas flow rate (L/min)	1	1
Liquid flow rate (mL/min)	0.5	0.1
Liquid tube ID (µm)	200	35
Gas annular OD (µm)	340	170
Gas annular ID (µm)	280	95

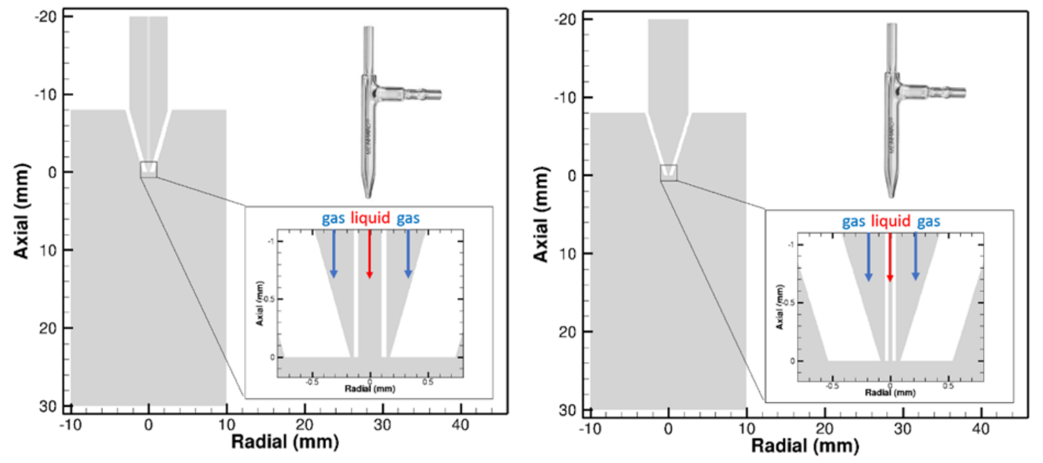

(a) (b)

Figure 1. The computational domain of two nebulizers with an axisymmetric configuration. (a) TR-50-A0.5, (b) HEN-90-A0.1

Gas flow field

The gas flow field was modelled with high-pressure gas and with no liquid flow. Due to the high pressure of the nebulizer gas, flow expansion and shock diamonds are formed in the wake of the annular nozzle flow with a Mach number up to 2. For a circular nozzle, the distance from the nozzle to the first shock diamond is commonly approximated by $x = 0.67\,D\sqrt{P_0/P_1}$. For the current annular nozzle, if the diameter term D in the above equation is replaced by the annular gap width, the calculated distance x for TR-50-A0.5 is 42 µm, while the calculated distance x for HEN-90-A0.1 is 134 µm. The simulation results shown in Figure 2 agree with the above calculations.

Figures 2 (a) and (b) display the velocity field for these two nebulizers. Nebulizer TR-50-A0.5 generates distinct shock diamonds in the wake flow up to 0.4 mm from the gas exit. Since the annular radius gap for gas flow in HEN-90-A0.1 is only slighter smaller than the gas tube inner radius, the shock waves from the annular orifice strongly interact with each other and gradually merge in the downstream wake flow up to a distance of 1.6 mm. A flow recirculation area with lower pressure is formed near the liquid orifice exit in both nebulizers, which contributes to gas entertainment for droplet generation.

Figure 3 plots temperature contours. The stronger flow expansion in HEN-90-A0.1 produces a lower temperature in the nebulizer wake flow, which is a disadvantage from the point of view of droplet evaporation in an electrospray MS ion source.

The Unsteady RANS simulation captures the vortex shedding frequency of turbulent flow from the annular orifice, which is approximately 12.5 kHz (a time cycle of 80 µs) for TR-50-A0.5 and 100 kHz (a time cycle of 10 µs) for HEN-90-A0.1. This frequency determines gas entrainment frequency for a flow-blurring nebulizer during the process of droplet generation.

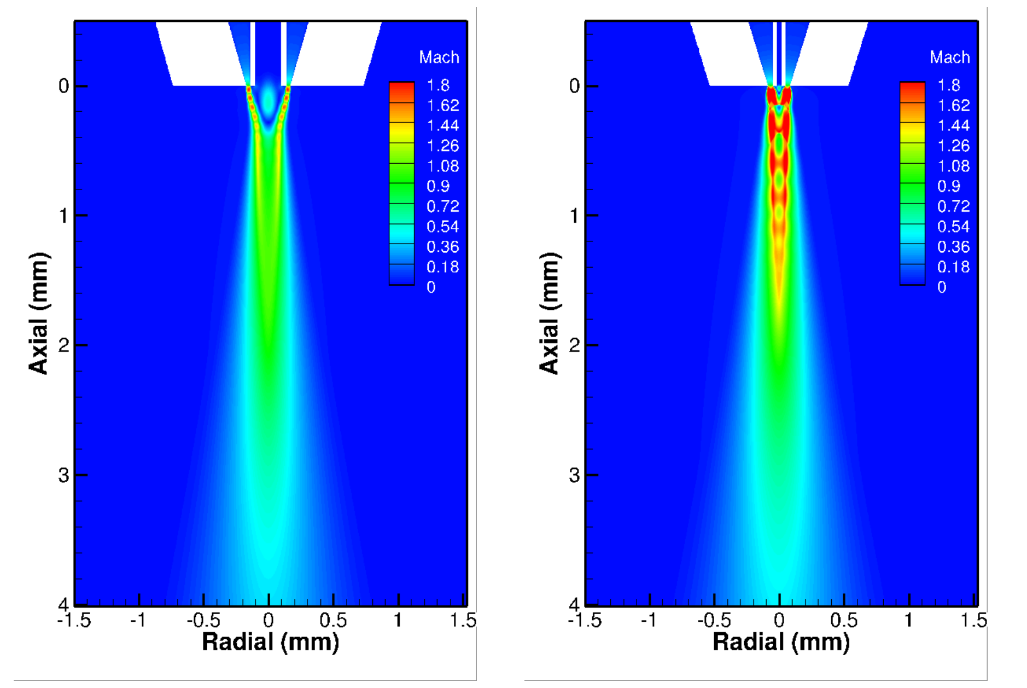

(a) (b)

Figure 2. Gas velocity field. (a)TR-50-A0.5, (b)HEN-90-A0.1

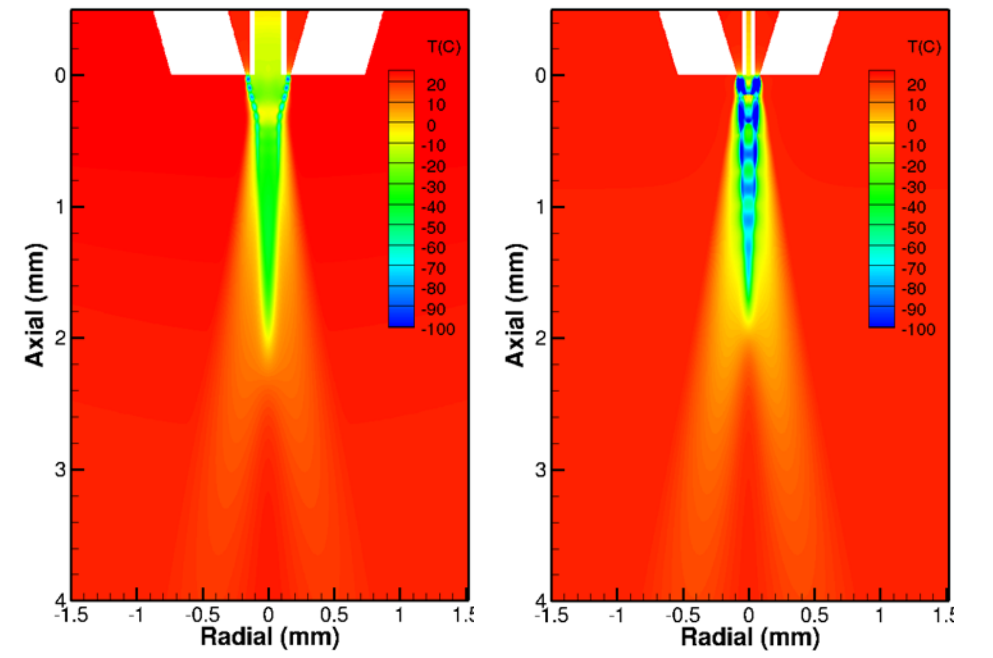

(a) (b)

Figure 3. Temperature field. (a) TR-50-A0.5, (b) HEN-90-A0.1

Dynamics of droplet generation

High-speed coaxial gas flow results in a dynamic change in the local liquid surface topology. The liquid firstly transfers into a liquid sheet, and then breaks up into ligament and droplets due to Kelvin-Helmholtz instability in the axial direction and Rayleigh-Taylor instability in the azimuthal direction [2].

Figure 4 illustrates a droplet production cycle for (a) TR-50-A0.5 and (b) HEN-90-A0.1. The cycle time is the same as the flow vortex shedding period, which can also be seen from the shown streamlines. Gas flow recirculation near the liquid exit introduces gas entrainment into the liquid tube which is a typical feature of flow blurring nebulizers [3]. This feature is clearly observed in TR-50-A0.5, but HEN-90-A0.1 only has very mild and shallow gas entrainment.

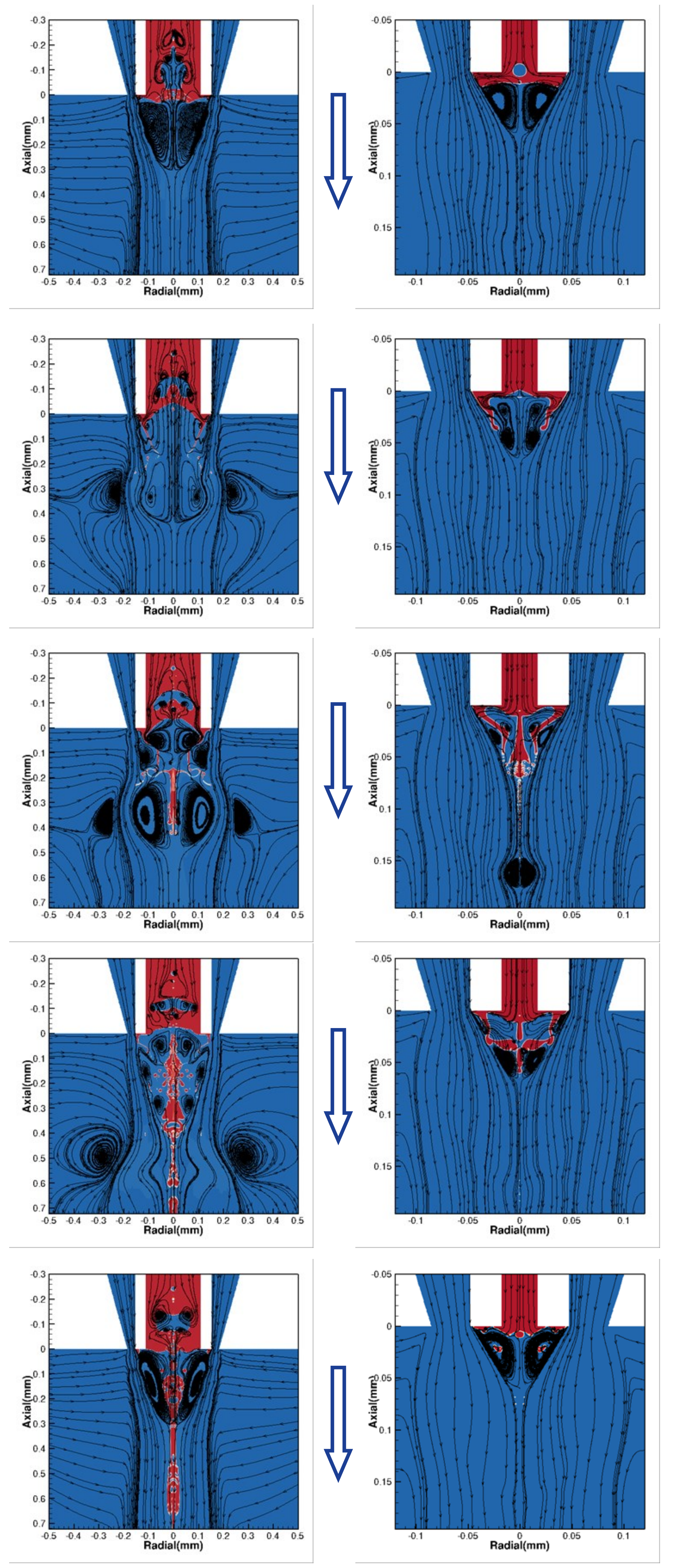

(a) (b)

Figure 4. Snapshot of a typical droplet generation cycle for (a) TR-50-A0.5 and (b) HEN-90-A0.1. Red color for liquid and blue for gas. Streamlines with directions are also shown.

Simulations also show that a typical liquid ligament length and diameter before breakup are approximately 180 µm and 15 µm for TR-50-A0.5, 60 µm and 6 µm for HEN-90-A0.1, respectively.

Figure 5 displays enlarged plots of primary droplets in TR-50-A0.5 and HEN-90-A0.1. Typical primary droplet sizes for TR-50-A0.5 are 5-10 µm and 2-4 µm for HEN-90-A0.1 for most of the generated droplets. The interaction between shock waves in the HEN-90-A0.1 introduces a quasi-impingement process in the droplet generation with small droplets both in the middle and edge of the plume [4]. For both nebulizers, large droplets move faster in the middle of the plume.

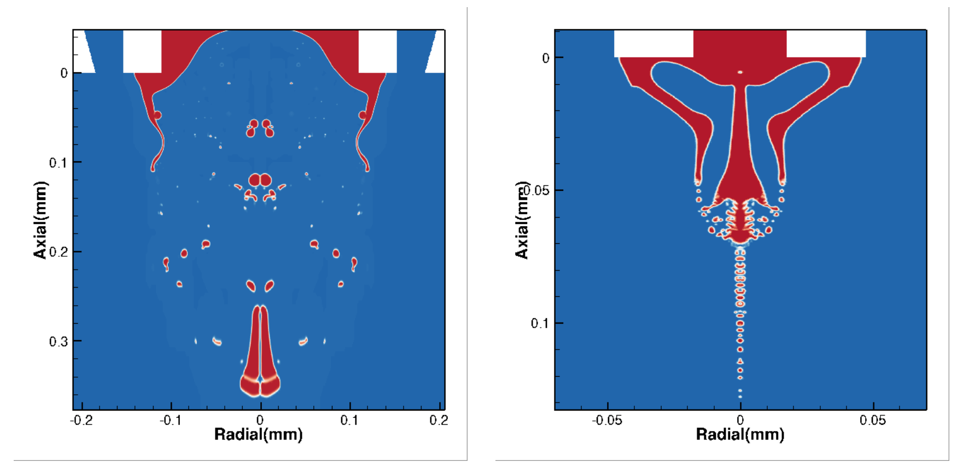

(a) (b)

Figure 5. Snapshot of primary droplet size and locations. (a) for TR-50-A0.5 (b) for HEN-90-A0.1

Droplet transport

The VOF method with adaptive mesh refinement demands a very high mesh resolution to capture the gas-liquid interface of microscale droplets. In order to reduce the calculation cost, a DPM method with an atomization model was validated for application in the high-speed nebulizers. Figure 6 (a) and Figure 7 (a) display the diameters of droplets in TR-50-A0.5 and HEN-90-A0.1, respectively.

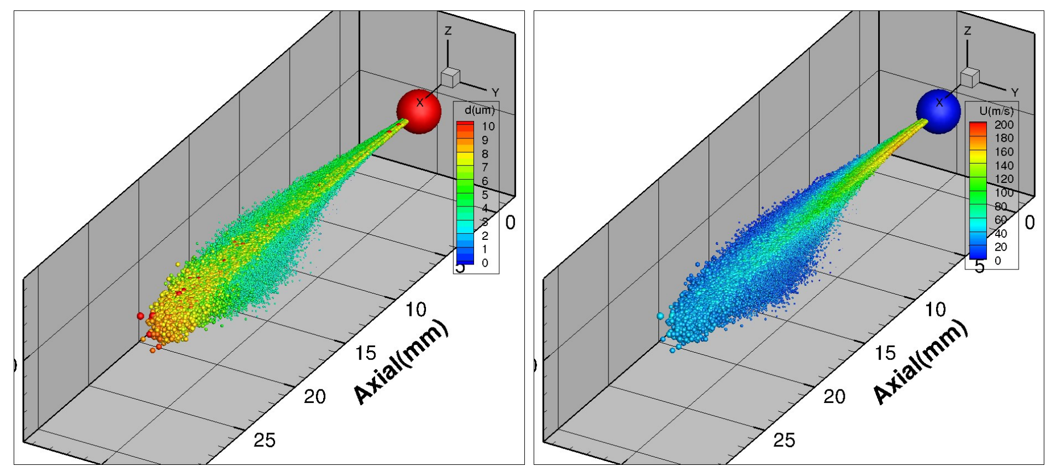

(a) (b)

Figure 6. Droplet transport in TR-50-A0.5 (droplets above z=0 are omitted for clarity). (a) colored by droplet diameter, (b) colored by droplet axial velocity

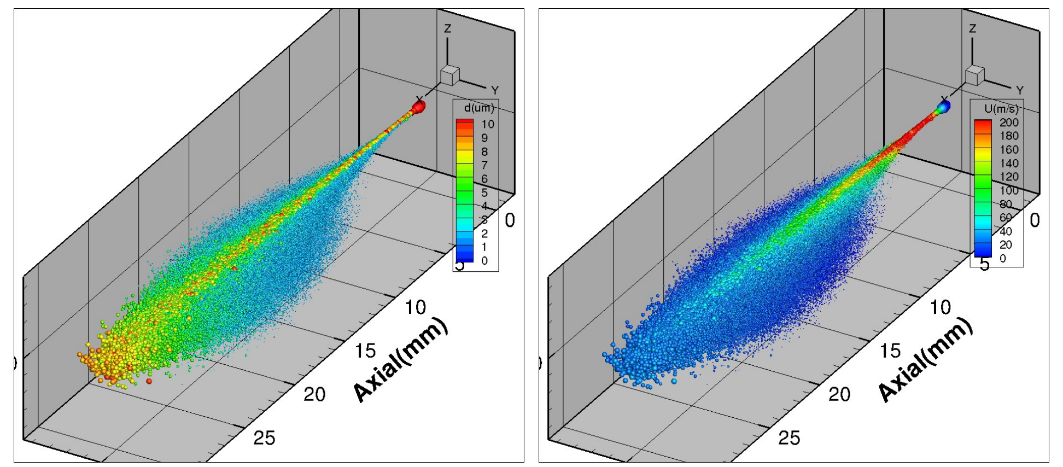

(a) (b)

Figure 7. Droplet transport in HEN-90-A0.1 (droplets above z=0 are omitted for clarity). (a) colored by droplet diameter, (b) colored by droplet axial velocity

It appears that HEN-90-A0.1 produces finer droplets in the plume at a given distance from the capillary. Both nebulizers produce larger droplets in the centre of the plumes. At around 20mm from the capillary, the plume width shrinks due to evaporation (and loss) of droplets. In this respect, the HEN-90-A0.1 has a wider plume than TR-50-A0.5 due to a lower residence time and reduced evaporation, although it has a narrower plume than TR-50-A0.5 at the initial stage. Figures 6 (b) and 7 (b) show the droplet velocities in the spray plumes. The higher gas velocity of HEN-90-A0.1 produces higher speed droplets in the middle of plume.

Compared to experimental measurements of droplet size distributions, the atomization model in ANSYS Fluent underestimates both D[3,2] and Dv50 diameters. The simulated relative span of the distribution is much smaller than the experimental measurement for both nebulizers. We believe that these current limitations are related to the low Weber numbers used in the empirical formulation of the sheet and ligament constants [5], which are well below the Weber numbers encountered for droplets in these nebulisers.

In order to overcome some of the limitations of the current two-stage atomization simulations, it is anticipated that a single, hybrid VOF to DPM model, which numerically converts generated droplets by VOF to tracked droplets by DPM, would more accurately predict the spray characteristics of high-velocity, air-blast nebulizers. This will form part of our future work.

CONCLUSION

- **Strong flow expansion occurs in both Meinhard® TR-50-A0.5 and HEN-90-A0.1 nebulizers up to 1 mm away from the gas flow orifice. The geometry of HEN-90-A0.1 introduces high interaction between shock diamonds.**
- **The stronger flow expansion in HEN-90-A0.1 also results in a lower temperature than TR-50-A0.5 in the key area of droplet formation.**
- **Droplet formation occurs at the same frequency as the gas flow vortex shedding, and the frequency in HEN-90-A0.1 is almost 80 times higher than that of TR-50-A0.5.**
- **Both nebulizers show flow-blurring in droplet generation, where liquid tube gas entrainment in TR-50-A0.5 is stronger.**
- **The VOF model shows that the majority of droplets generated by HEN-90-A0.1 have almost half the diameter of droplets generated by TR-50-A0.5.**
- **The atomization model in the DPM method can only capture qualitative properties of droplet transport, and underestimates both droplet diameters and droplet distribution widths.**

References

1. https://www.meinhard.com

2. D. Kim and P. Moin, “Numerical simulation of the breakup of a round liquid jet by a coaxial flow of gas with a subgrid Lagrangian breakup model,” Center for Turbulence Research, Annual Research Briefs, 2011.

3. Gañán-Calvo, Alfonso M. "Enhanced liquid atomization: From flow-focusing to flow-blurring." Applied Physics Letters 86.21 (2005): 214101.

4. Etzold, Mathias, Gerald Betz, and Franz Durst. "Twin-jet Spray and Drop-impingement Spray Injectors for Engine Applications." MTZ worldwide 79.12 (2018): 54-59.

5. ANSYS Fluent Theory Guide, ANSYS, Inc., 275 Technology Drive Canonsburg,. PA 15317, November 2018